Black phosphorus as saturable absorber for the Q-switched Er:ZBLAN fiber laser at 2.8 µm

Zhipeng Qin,[1] Guoqiang Xie,[1,4] Han Zhang,[2] Chujun Zhao,[3,5] Peng Yuan,[1] Shuangchun Wen,[3] and Liejia Qian[1]

[1]*Key Laboratory for Laser Plasmas (Ministry of Education), Department of Physics and Astronomy, IFSA Collaborative Innovation Center, Shanghai Jiao Tong University, Shanghai 200240, China*
[2]*SZU-NUS Collaborative Innovation Center for Optoelectronic Science & Technology, Key Laboratory of Optoelectronic Devices and Systems of Ministry of Education and Guangdong Province, College of Optoelectronic Engineering, Shenzhen University, Shenzhen 518060, China*
[3]*Key Laboratory for Micro-/Nano-OptoelectronicDevices of Ministry of Education, School of Physics and Electronics, Hunan University, Changsha 410082, China*
[4]*xiegq@sjtu.edu.cn*
[5]*cjzhao@hnu.edu.cn*

Abstract: Black phosphorus, a newly emerged two-dimensional material, has attracted wide attention as novel photonic material. Here, multilayer black phosphorus is successfully fabricated by liquid phase exfoliation method. By employing black phosphorus as saturable absorber, we demonstrate a passively Q-switched Er-doped ZBLAN fiber laser at the wavelength of 2.8 μm. The modulation depth and saturation fluence of the black phosphorus saturable absorber are measured to be 15% and 9 μJ/cm^2, respectively. The Q-switched fiber laser delivers a maximum average power of 485 mW with corresponding pulse energy of 7.7 μJ and pulse width of 1.18 μs at repetition rate of 63 kHz. To the best of our knowledge, this is the first time to demonstrate that black phosphorus can realize Q-switching of 2.8-μm fiber laser. Our research results show that black phosphorus is a promising saturable absorber for mid-infrared pulsed lasers.

OCIS codes: (140.3380) Laser materials; (140.3540) Lasers, Q-switched; (140.3070) Infrared and far-infrared lasers.

References and links

1. K. S. Novoselov, A. K. Geim, S. V. Morozov, D. Jiang, Y. Zhang, S. V. Dubonos, I. V. Grigorieva, and A. A. Firsov, “Electric field effect in atomically thin carbon films,” Science **306**(5696), 666–669 (2004).
2. A. K. Geim, “Graphene: status and prospects,” Science **324**(5934), 1530–1534 (2009).
3. J. E. Moore, “The birth of topological insulators,” Nature **464**(7286), 194–198 (2010).
4. H. Zhang, C. Liu, X. Qi, X. Dai, Z. Fang, and S. Zhang, “Topological insulators in Bi_2Se_3, Bi_2Te_3 and Sb_2Te_3 with a single Dirac cone on the surface,” Nat. Phys. **5**(6), 438–442 (2009).
5. A. A. Al-Hilli and B. L. Evans, “The preparation and properties of transition metal dichalcogenide single crystals,” J. Cryst. Growth **15**(2), 93–101 (1972).
6. A. Ayari, E. Cobas, O. Ogundadegbe, and M. S. Fuhrer, “Realization and electrical characterization of ultrathin crystals of layered transition-metal dichalcogenides,” J. Appl. Phys. **101**(1), 014507 (2007).
7. K. F. Mak, M. Y. Sfeir, Y. Wu, C. H. Lui, J. A. Misewich, and T. F. Heinz, “Measurement of the optical conductivity of graphene,” Phys. Rev. Lett. **101**(19), 196405 (2008).
8. J. M. Dawlaty, S. Shivaraman, M. Chandrashekhar, F. Rana, and M. G. Spencer, “Measurement of ultrafast carrier dynamics in epitaxial graphene,” Appl. Phys. Lett. **92**(4), 042116 (2008).
9. T. J. Echtermeyer, L. Britnell, P. K. Jasnos, A. Lombardo, R. V. Gorbachev, A. N. Grigorenko, A. K. Geim, A. C. Ferrari, and K. S. Novoselov, “Strong plasmonic enhancement of photovoltage in graphene,” Nat. Commun. **2**, 458 (2011).
10. B. Radisavljevic, A. Radenovic, J. Brivio, V. Giacometti, and A. Kis, “Single-layer MoS_2 transistors,” Nat. Nanotechnol. **6**(3), 147–150 (2011).
11. M. Liu, X. Yin, E. Ulin-Avila, B. Geng, T. Zentgraf, L. Ju, F. Wang, and X. Zhang, “A graphene-based broadband optical modulator,” Nature **474**(7349), 64–67 (2011).
12. J. Ma, G. Xie, P. Lv, W. Gao, P. Yuan, L. Qian, U. Griebner, V. Petrov, H. Yu, H. Zhang, and J. Wang, “Wavelength-versatile graphene-gold film saturable absorber mirror for ultra-broadband mode-locking of bulk lasers,” Sci. Rep. **4**, 5016 (2014).

#246936 Received 29 Jul 2015; revised 5 Sep 2015; accepted 6 Sep 2015; published 10 Sep 2015

13. Y. Zhang, S. Wang, H. Yu, H. Zhang, Y. Chen, L. Mei, A. Di Lieto, M. Tonelli, and J. Wang, "Atomic-layer molybdenum sulfide optical modulator for visible coherent light," Sci. Rep. **5**, 11342 (2015).
14. C. Zhao, Y. Zou, Y. Chen, Z. Wang, S. Lu, H. Zhang, S. Wen, and D. Tang, "Wavelength-tunable picosecond soliton fiber laser with Topological Insulator: Bi_2Se_3 as a mode locker," Opt. Express **20**(25), 27888–27895 (2012).
15. J. Ma, G. Q. Xie, P. Lv, W. L. Gao, P. Yuan, L. J. Qian, H. H. Yu, H. J. Zhang, J. Y. Wang, and D. Y. Tang, "Graphene mode-locked femtosecond laser at 2 μm wavelength," Opt. Lett. **37**(11), 2085–2087 (2012).
16. Z. Luo, Y. Huang, J. Weng, H. Cheng, Z. Lin, B. Xu, Z. Cai, and H. Xu, "1.06 μm Q-switched ytterbium-doped fiber laser using few-layer topological insulator Bi_2Se_3 as a saturable absorber," Opt. Express **21**(24), 29516–29522 (2013).
17. Z. Luo, C. Liu, Y. Huang, D. Wu, J. Wu, H. Xu, Z. Cai, Z. Lin, L. Sun, and J. Weng, "Topological-insulator passively Q-switched double-clad fiber laser at 2 μm wavelength," IEEE J. Sel. Top. Quantum Electron **20**(5), 0902708 (2014).
18. Q. H. Wang, K. Kalantar-Zadeh, A. Kis, J. N. Coleman, and M. S. Strano, "Electronics and optoelectronics of two-dimensional transition metal dichalcogenides," Nat. Nanotechnol. **7**(11), 699–712 (2012).
19. A. N. Abbas, B. Liu, L. Chen, Y. Ma, S. Cong, N. Aroonyadet, M. Köpf, T. Nilges, and C. Zhou, "Black phosphorus gas sensors," ACS Nano **9**(5), 5618–5624 (2015).
20. L. Li, Y. Yu, G. J. Ye, Q. Ge, X. Ou, H. Wu, D. Feng, X. H. Chen, and Y. Zhang, "Black phosphorus field-effect transistors," Nat. Nanotechnol. **9**(5), 372–377 (2014).
21. J. Dai and X. C. Zeng, "Bilayer phosphorene: effect of stacking order on bandgap and its potential applications in thin-film solar cells," J. Phys. Chem. Lett. **5**(7), 1289–1293 (2014).
22. H. Liu, Y. Du, Y. Deng, and P. D. Ye, "Semiconducting black phosphorus: synthesis, transport properties and electronic applications," Chem. Soc. Rev. **44**(9), 2732–2743 (2015).
23. V. Tran, R. Soklaski, Y. Liang, and L. Yang, "Layer-controlled band gap and anisotropic excitons in few-layer black phosphorus," Phys. Rev. B **89**(23), 235319 (2014).
24. J. Qiao, X. Kong, Z. X. Hu, F. Yang, and W. Ji, "High-mobility transport anisotropy and linear dichroism in few-layer black phosphorus," Nat. Commun. **5**, 4475 (2014).
25. Y. Chen, G. Jiang, S. Chen, Z. Guo, X. Yu, C. Zhao, H. Zhang, Q. Bao, S. Wen, D. Tang, and D. Fan, "Mechanically exfoliated black phosphorus as a new saturable absorber for both Q-switching and Mode-locking laser operation," Opt. Express **23**(10), 12823–12833 (2015).
26. S. B. Lu, L. L. Miao, Z. N. Guo, X. Qi, C. J. Zhao, H. Zhang, S. C. Wen, D. Y. Tang, and D. Y. Fan, "Broadband nonlinear optical response in multi-layer black phosphorus: an emerging infrared and mid-infrared optical material," Opt. Express **23**(9), 11183–11194 (2015).
27. Z. Luo, M. Liu, Z. Guo, X. Jiang, A. Luo, C. Zhao, X. Yu, W. Xu, and H. Zhang, "Microfiber-based few-layer black phosphorus saturable absorber for ultra-fast fiber laser," Opt. Express **23**(15), 20030–20039 (2015).
28. R. Zhang, Y. Zhang, H. Yu, H. Zhang, R. Yang, B. Yang, Z. Liu, and J. Wang, "Broadband black phosphorus optical modulator in visible to mid-infrared spectral range," arXiv:1505.05992 (2015).
29. D. Li, H. Jussila, L. Karvonen, G. Ye, H. Lipsanen, X. Chen, and Z. Sun, "Ultrafast pulse generation with black phosphorus," arXiv:1505.00480 (2015).
30. T. Jiang, K. Yin, X. Zheng, H. Yu, and X. Cheng, "Black phosphorus as a new broadband saturable absorber for infrared passively Q-switched fiber laser," arXiv:1504.07341 (2015).
31. C. Wei, X. Zhu, F. Wang, Y. Xu, K. Balakrishnan, F. Song, R. A. Norwood, and N. Peyghambarian, "Graphene Q-switched 2.78 μm Er^{3+}-doped fluoride fiber laser," Opt. Lett. **38**(17), 3233–3236 (2013).
32. J. Li, H. Luo, L. Wang, C. Zhao, H. Zhang, H. Li, and Y. Liu, "3-μm mid-infrared pulse generation using topological insulator as the saturable absorber," Opt. Lett. **40**(15), 3659–3662 (2015).
33. J. Li, H. Luo, L. Wang, B. Zhai, H. Li, and Y. Liu, "Tunable Fe^{2+}:ZnSe passively Q-switched Ho^{3+}-doped ZBLAN fiber laser around 3 μm," Opt. Express **23**(17), 22362–22370 (2015).
34. J. F. Li, H. Y. Luo, Y. L. He, Y. Liu, L. Zhang, K. M. Zhou, A. G. Rozhin, and S. K. Turistyn, "Semiconductor saturable absorber mirror passively Q-switched 2.97 μ m fluoride fiber laser," Laser Phys. Lett. **11**(6), 065102 (2014).

1. Introduction

Rapid progress has been made on two-dimensional (2D) materials represented by graphene, topological insulators (TIs) and transition metal dichalcogenides (TMDCs) in recent years [1–6]. Due to their broadband absorption, ultrafast carrier dynamics and planar characteristics [7, 8], they have been regarded as the next-generation optoelectronics devices such as photoelectric detector, field-effect transistor, optical modulator, and so on [9–11]. So far, Q-switched and mode-locked lasers have been frequently reported with 2D materials as saturable absorber (SA) [12–17]. In the family of 2D materials, graphene is characterized by zero-bandgap which makes it have extremely broadband optical response from visible to mid-infrared (mid-IR) band [12]. However, its weak absorption results in a low modulation depth [15]. TIs are characterized by a full insulating gap in the bulk and gapless edge or surface states and TI SAs mainly work at 1, 1.5 and 2 μm wavelength at present [14, 16, 17]. TMDCs such as MoS_2 and WS_2 generally have large bandgap (1~2 eV) [13, 18], which limits their applications in the mid-IR wavelength.

Black phosphorus (BP), a newly emerged 2D material, has gained wide attention recently. Up to now, it has been reported that BP can be applied in sensor, field-effect transistor and solar cell [19–21]. Multilayer BP has a similar structure with bulk graphite. In a single layer, each phosphorus atom is covalently bonded with three adjacent phosphorus atoms to form a puckered honeycomb structure, and different layers are stacked together by van der Waals interaction [22]. Multilayer BP has a direct energy bandgap structure, with bandgap from 0.3 eV to 2 eV depending on the number of layers [23]. Naturally, BP has the common properties of 2D materials such as wideband absorption, ultrafast carrier dynamics and planar characteristic [24]. The bandgap-controllable BP SA can be fabricated by mechanical exfoliation method or liquid phase exfoliation (LPE) method [25, 26]. So far, the saturable absorption of BP has been demonstrated experimentally by Q-switched or mode-locked lasers from 0.6 to 2.0 μm wavelength [27–30]. However, there is no report on BP for Q-switched lasers at the wavelength of 2.8 μm. In this spectral regime, passively Q-switched fiber lasers have been achieved recently by graphene, TI, Fe:ZnSe, and semiconductor saturable absorber mirror (SESAM) [31–34]. Compared with BP, the zero-bandgap structure of graphene weakens the absorption at long wavelength, and TI, Fe:ZnSe, and SESAM need complex fabrication process.

Here we experimentally demonstrate that BP SA is also feasible at the wavelength of 2.8 μm. The multilayer BP, prepared by LPE method, was coated on a gold-coated mirror as reflection-type saturable absorber mirror (SAM). By employing the fabricated BP-SAM, we demonstrated a passively Q-switched Er-doped ZBLAN fiber laser at 2.8 μm. The Q-switched fiber laser delivered a maximum average power of 485 mW with corresponding pulse energy of 7.7 μJ and pulse width of 1.18 μs at repetition rate of 63 kHz. Due to the strong water absorption in body tissue for 3 μm laser, 3-μm pulsed laser is very useful in medical applications such as skin ablation, dentistry and cataract, etc.

2. Preparation and characterization of BP SA

In this work, the multilayer BP was prepared by LPE method, which has been widely used to obtain 2D nanomaterials from layered bulk crystal. Firstly, we mixed bulk black phosphorous (30 mg) with N-Methyl pyrrolidone (NMP) solution (30 mL) together and sonicated at 40 kHz frequency and 300 W power for 10 hours. Then, the supernatant liquor was obtained after centrifuging at 1500 rpm for 10 min. The detailed characterization of transmission electron microscopy (TEM) and atomic force microscopy (AFM) with same BP sample was performed in [26], which suggested that the multilayer BP flakes had a thickness distribution from ~5 nm-20 nm, and more than 51% of the flakes had an thickness between 15 nm and 20 nm [26]. Since the bandgap of BP follows a power law $Eg \approx (1.7/n^{0.73} + 0.3)$ eV (n is the number of layers) [23], the bandgap of the multilayer BP should be larger than 0.432 eV, corresponding to an optical wavelength upper limit of ~2.9 μm. In the experiment, the as-prepared BP-NMP solution (supernatant liquor) was dropped onto gold-coated mirror and dried in cabinet for laser experiment. In combination with the ultra-broadband gold-coated reflective mirror, the fabricated BP-SAM can operate in a broad spectral range (<2.9 μm). It is noticed that BP flakes on the mirror are not uniform according to the TEM image [26]. The reflectivity of the BP-SAM was measured to be ~79% with a 2.8 μm continuous-wave (CW) laser. The saturable absorption of the BP-SAM was measured with a home-made mode-locked fiber laser at the wavelength of 2.8 μm, as shown in Fig. 1. The mode-locked laser delivered a maximum average output power of 1.05 W with a repetition rate of 22.56 MHz and pulse duration of 25 ps. By changing the incident fluence, the reflectivity of BP-SAM increased from 79% to 91%. The measurement shows that the BP-SAM has a modulation depth of 15% and saturation fluence of 9 $\mu J/cm^2$ at 2.8 μm.

#246936 Received 29 Jul 2015; revised 5 Sep 2015; accepted 6 Sep 2015; published 10 Sep 2015

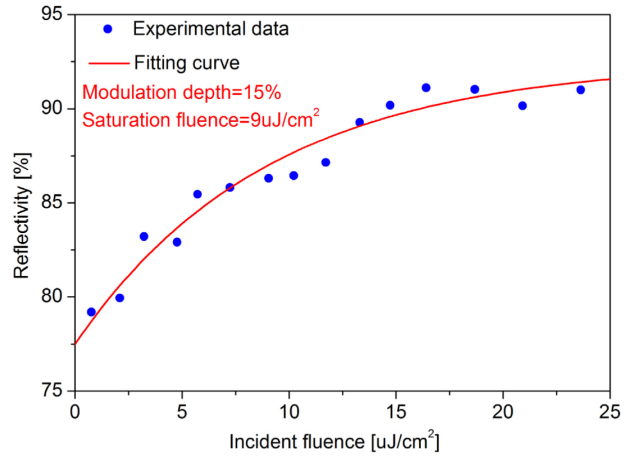

Fig. 1. The saturable absorption measurement of BP-SAM at 2.8 μm wavelength.

3. Experimental setup

The schematic of the Q-switched fiber laser is shown in Fig. 2. The commercialized 976-nm laser diode (BTW, Beijing) was adopted as the pump source with maximum output power of 30 W, a core diameter of 105 μm and numerical aperture (NA) of 0.15. After collimated by a biconvex lens (F1 = 50 mm), the pump light was focused into first cladding configuration by the second biconvex lens (F2 = 100 mm). The 45° placed quartz mirror was antireflectively coated for pump light (T>95%) and highly reflectively coated for laser (R>99%). The double-cladding Er:ZBLAN fiber (FiberLabs, Japan) has a length of 4 m and Er-doping concentration of 6 mol.%. The core diameter of Er:ZBLAN fiber is 30 μm with NA of 0.12. The first cladding configuration has a diameter of 300 μm and NA of 0.5, which guarantees efficient coupling of pump light. The pumping end facet of fiber was cut perpendicular to the fiber axis, with a Fresnel transmission of 96% as output coupler. At the tail end of fiber, it was cut with an angle of 8° to avoid parasitic oscillation. Then, two highly-reflective plane-convex mirrors (M1 and M2) with radii of curvature of 100 mm and 50 mm respectively, were used to reimage the end face of fiber onto BP-SAM. The laser mode on the BP-SAM was half of fiber core diameter.

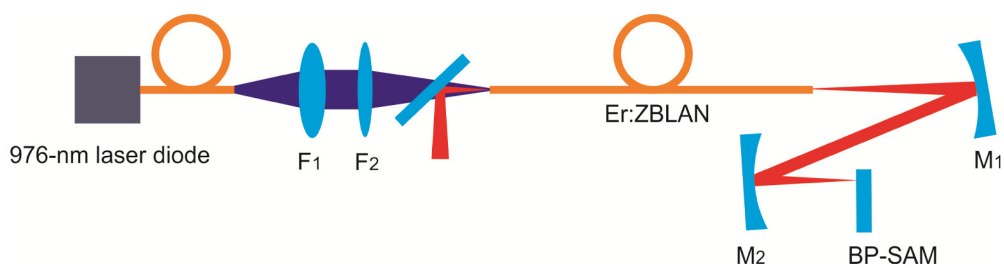

Fig. 2. The schematic of the passively Q-switched Er:ZBLAN fiber laser. BP-SAM, black phosphorus saturable absorber mirror.

4. Experimental results and discussion

With the laser setup of Fig. 2, CW laser was generated at the threshold of incident pump power of 1.4 W. When the incident pump power increased to 2.2 W, the fiber laser started Q-switching operation. In the experiment the pulse train was captured by an infrared HgCdTe detector with a specified rise time of < 2 ns and working wavelength range of 1~9 μm (VIGO System model PCI-9), and displayed in a digital oscilloscope with 500-MHz bandwidth

#246936 Received 29 Jul 2015; revised 5 Sep 2015; accepted 6 Sep 2015; published 10 Sep 2015

(Tektronix, DPO3054). The typical Q-switched pulse trains and pulse profiles are shown in Fig. 3 for different pump powers. At the Q-switching threshold, the fiber laser had an average output power of 145 mW, pulse width of 2.1 μs and repetition rate of 39 kHz. The Q-switching operation can be maintained when the incident pump power increased continuously. For incident pump power of 3.8 W, the average output power reached to 320 mW with a pulse width of 1.35 μs and repetition rate of 54 kHz. The shortest pulse width of 1.18 μs was obtained with an average output power of 485 mW and repetition rate of 63 kHz under an incident pump power of 5.4 W. In high power operation, the Q-switched pulses show slight intensity fluctuation, which may be attributed to BP performance degradation due to excess heat. The radio-frequency (RF) spectrum was measured under the maximum output power, as shown in the inset of Fig. 3d, which shows a signal-to-noise ratio (SNR) of 35 dB. It was worth noting that the position of BP-SAM was a key factor for Q-switching operation. In the experiment we carefully optimized the BP-SAM position for achieving the maximum output power and Q-switching operation.

The Q-switched average output power and pulse energy as a function of incident pump power is shown in Fig. 4(a). The average output power increased linearly from 145 mW to 485 mW with a slope efficiency of 10.6%. At the maximum output power of 485 mW in Q-switched regime, we obtained the maximum pulse energy of 7.7 μJ. Figure 4(b) shows the measured repetition rate and pulse width as a function of incident pump power. As expected, the repetition rate increased and pulse width decreased as the incident pump power increased. The repetition rate increased from 39 kHz to 63 kHz and pulse width decreased from 2.10 μs to 1.18 μs while the incident pump power varied from 2.2 W to 5.4 W. In the experiment, no Q-switched mode-locking phenomenon was observed.

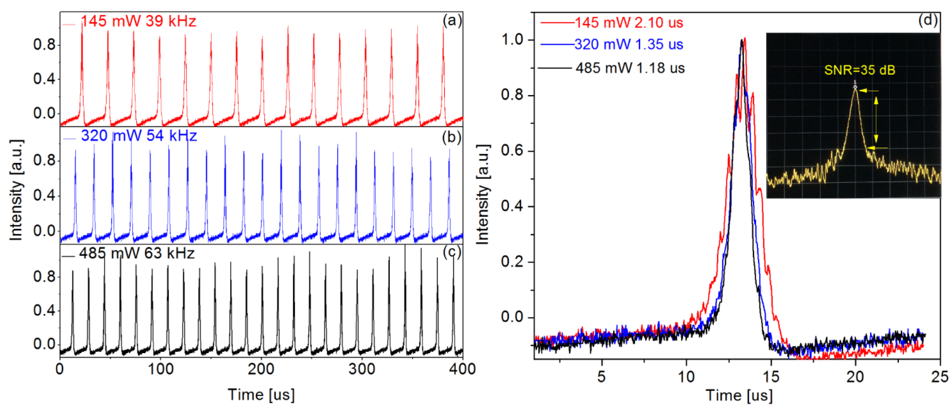

Fig. 3. (a-c) Q-switched pulse trains at the output powers of 145 mW, 320 mW and 485 mW, respectively. (d) Their corresponding pulse profiles and the RF spectrum.

#246936 Received 29 Jul 2015; revised 5 Sep 2015; accepted 6 Sep 2015; published 10 Sep 2015

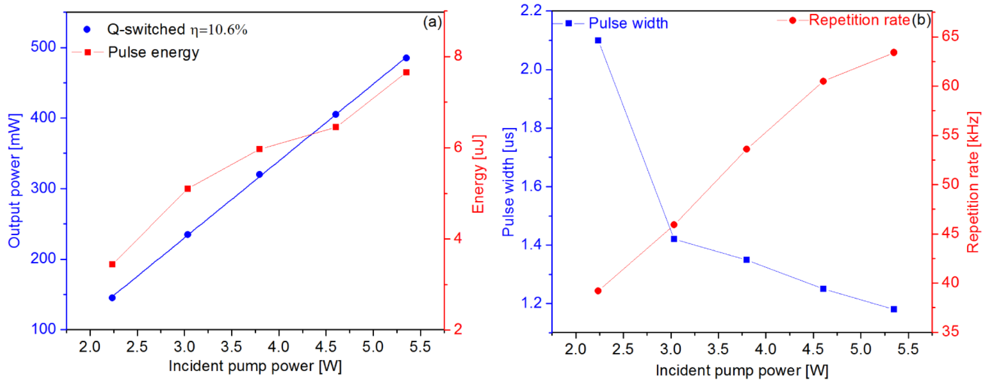

Fig. 4. (a) Average output power and pulse energy, (b) Repetition rate and pulse width as a function of incident pump power.

Figure 5 shows the Q-switched pulse spectrum, which was measured by a mid-IR spectral analyzer (Ocean Optics, SIR 5000) with a resolution of 0.22 nm. The spectral peak locates at 2779 nm with a FWHM of 4.6 nm.

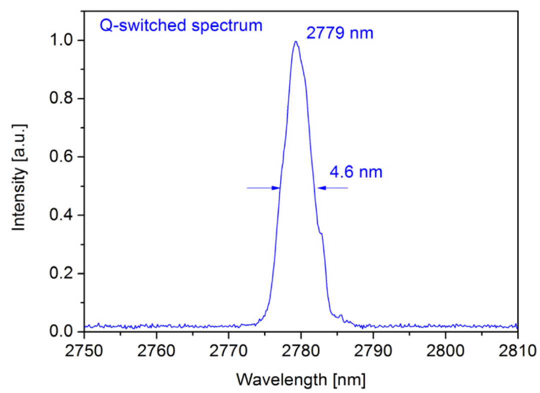

Fig. 5. The Q-switched pulse spectrum measured at the maximum output power.

5. Conclusion

In conclusion, multilayer BP was fabricated by LPE method and the 2.8 μm Q-switched fiber laser was experimentally demonstrated with BP as saturable absorber for the first time. The Q-switched fiber laser delivered a maximum average output power of 485 mW with pulse energy of 7.7 μJ, pulse width of 1.18 μs and repetition rate of 63 kHz. The BP is of low cost, easy fabrication, and variable bandgap, which makes it potential as a broadband saturable absorber for pulsed lasers, especially in the mid-IR spectral regime where few saturable absorbers can work stably.

Acknowledgment

The work is partially supported by Shanghai Excellent Academic Leader Project (Grant No. 15XD1502100), National Basic Research Program of China (Grant No. 2013CBA01505) and National Natural Science Foundation of China (Grant No. 11421064).